

Risk-based flood adaptation assessment for large-scale buildings in coastal cities using cloud computing

Yu Han^{a,*}, Pallab Mozumder^{a,b}

^a Institute of Environment, Department of Earth & Environment, Florida International University, Miami, FL, 33199, USA

^b Department of Economics, Florida International University, Miami, FL, 33199, USA

ARTICLE INFO

Keywords:

Sea-level rise
Decision-making
Cloud computing
Adaptation
Sensitivity analysis

ABSTRACT

Flood risk management (FRM) in coastal cities is a challenging task due to uncertain climate hazards under sea-level rise (SLR) and large-scale vulnerable buildings within in the floodplain. This study presents a building-level adaptation framework to evaluate alternative community adaptation strategies relying on cloud computing. We incorporated multiple sources of model uncertainties and randomly generated storm surges in each year of simulation using the extreme value distribution (GEV) theory. Based on a case study in Miami-Dade County, Florida, four adaptation scenarios were designed to evaluate their effectiveness in adaptation. Our sensitivity analysis suggested a positive linear relationship between community flood risk reduction and total community adaptation costs in the life-cycle cost-benefit (LCCB) model. Our results showed that uncertainties of the total community damage based on the LCCB model ranges from \$221 million to \$2.75 billion. However, when considering social vulnerability, the total community damage increased substantially, ranging from \$244 million to \$3.44 billion. Nevertheless, a 6ft public seawall based on the upper bound of the GEV distribution with the enforced building elevation policy in flood zones could substantially reduce community flood damage under uncertain sea-level rises.

1. Introduction

Over the past decades, flood related hazards are among the most expensive natural disasters which caused loss of life, damage of buildings, and deterioration of the urban ecosystems. Given the compound effects of increasingly vulnerable human habitats and climate change, threats of flooding could be exacerbated. For example, building damages from hurricane Sandy (2012) and hurricane Harvey (2018) were both over billions of dollars (NCEI, 2021). The effects of sea-level rise (SLR) in coastal areas could further decrease the freeboard between the minimum building elevations in flood prone areas maintained by Federal Emergency Management (FEMA) and high water levels from king tides and storm surges, and thus increase the impacts of extreme weather events (Rahmstorf et al., 2007).

Given to high uncertainties of SLR, two approaches, a top-down approach and a bottom-up approach, are commonly used for risk assessment of buildings and infrastructures (Yang & Frangopol, 2020). The top-down approach relies on one or more climate and socioeconomic factors to assess community and infrastructure risk at local scales. For example, Martínez-Graña et al. (2018) qualitatively evaluated local

flood vulnerability due to SLR in Spain using geospatial techniques and a flood vulnerability index derived from multiple geophysical factors. Lyu, Zhou, Shen, and Zhou (2020) assessed inundation risk of the metro system in Shenzhen of China using an analytic hierarchy process method. Although the top-down risk assessment approach could identify risk and vulnerabilities from climate change, the method is not suitable for risk-based adaptation decision-making owing to large uncertainties of identified risk. By contrast, a bottom-up approach could examine the sensitivity of life-cycle risk of individual buildings or infrastructures to different climate-related parameters in adaptation planning. Therefore, a bottom-up approach with life-cycle risk management is particularly useful for risk-informed adaptation planning and to improve risk communication between the private and public sectors (Han & Mozumder, 2021).

Although many studies have been proposed in attempts to mitigate risk of buildings to climate disasters (W. Chen & Zhang, 2021; Y. Dong & Frangopol, 2017; Torabi, Dedekorkut-Howes, & Howes, 2018), due to high computational burden, few studies have been conducted to deal with large-scale building-level adaptation under uncertain climate disasters. Therefore, to improve public awareness of flood risk and

* Corresponding author at: Institute of Environment, Department of Earth & Environment, Florida International University, Miami, FL, 33199, USA.

E-mail address: hanyu.bit@gmail.com (Y. Han).

adaptation benefits, this paper presents a risk-based framework that utilizes cloud computing to examine flood exposure and vulnerability of large-scale buildings in cities and evaluates their adaptation benefits. Based on a case study in Miami-Dade County, Florida, flood damages of buildings are evaluated through stochastic storm surges under SLR projections. Our implemented simulation model could evaluate flood risk of large-scale buildings under SLR and improve risk communications in adaptation planning by incorporating climate and adaptation cost information from different sources. In the following section, we first presented a literature review, and then the methods to estimate building flood damages, life-cycle cost and benefit analysis model, designed adaptation scenarios, and the cloud-based model framework. Afterward, we introduced the case study area and explained model results based on large number of random simulations. Finally, we discussed main findings and limitations in this research.

2. Literature Review

Long-term SLR and coastal flood hazard have been recognized to produce highly consequential flood risk to coastal cities in the US and throughout the world (W. Sweet et al., 2017). Traditionally, the generalized extreme value (GEV) distribution theory is widely used for frequency-based coastal flood risk analysis (NOAA, 2013). However, given uncertainties of SLR, the GEV distribution is nonstationary. Lee, Haran, and Keller (2017) proposed four types of generalized extreme value distribution to assess storm surge events under climate change: a stationary GEV distribution with constant location, scale, and shape parameters, a nonstationary GEV distribution with only location parameter, a nonstationary GEV distribution with location and scale parameter, and a nonstationary GEV distribution with location, scale, and shape parameters. Recently, Ghanbari, Arabi, Obeyseker, and Sweet (2019) utilized a mixed normal-Generalized Pareto Distribution (GPD) distribution to evaluate coastal flood frequency under nonstationary conditions. Risk analysis of coastal flooding based on the GEV distributions also needs to be mapped to low lying areas to reflect local flood inundation conditions of communities. Although complex hydraulic and geomorphic models could more accurately simulate hydrodynamic and morpho-dynamic processes of storm surges, they usually include more variables and have their own assumptions. Therefore, given high uncertainties of flood mapping, the National Oceanic and Atmospheric Administration (NOAA) suggests a bathtub model using derived elevation data and tidal surface for flood planning (NOAA, 2010). Uncertainties of local tidal elevations and digital elevation model (DEM) are two main kinds of uncertainties involved in the bathtub model.

Coastal infrastructures and buildings are subject to the increasing flood vulnerability over the course of their service life due to SLR (Buchanan et al., 2020; Najafi, Zhang, & Martyn, 2021). However, the impacts of SLR on coastal communities are not homogeneous on the spatial-temporal scales due to complex environmental and socioeconomic factors. For example, due to the enforced adaptation policy within flood zones, McAlpine and Porter (2018) found that residential buildings that are outside flood zones in low-lying areas will face more flood damage than buildings in other locations under SLR.

The development of economic adaptation and risk mitigation strategies to cope with the increasing flood risk have been seen as an important investment approach to solve potential environmental, ecological, and social issues of flooding (Sampei Yamashita, Ryoichi Watanabe, & Shimatani, 2016). Cost-benefit analysis (CBA) is a commonly used approach to quantitatively evaluate total costs and benefits of a risk mitigation investment through an economic perspective during its full life-cycle (Pour, Wahab, Shahid, Asaduzzaman, & Dewan, 2020). Cutler, Albert, and White (2020) presented a dynamic CBA model by integrating shoreline erosion, coastal development, and adaptation into the evaluation of physical and economic interactions under SLR. Based on a discrete dynamic programming

method for evaluating adaptation decisions, they showed tradeoffs between adaptation and managed retreat under uncertain SLR.

Since adaptation decisions based on CBA are usually for the long-term trade-offs of economic costs and environmental benefits, these decisions are very sensitive to SLR impacts (Marangoni, Lamontagne, Quinn, Reed, & Keller, 2021). As a result, decisions of infrastructure adaptation and risk mitigation need to consider climate uncertainties (Hallegatte, 2009). Helmrich and Chester (2020) discussed different infrastructure adaptation frameworks accounting for future uncertainties of climate change. Garner, Reed, and Keller (2016) also pointed out the importance of quantifying tradeoffs of different policy objectives to better inform alternative climate risk mitigation policies.

Due to variations of SLR and coastal hazards, how and when to adapt to SLR related flood risk is challenging for stakeholders in coastal communities. Sahin and Mohamed (2013) introduced a spatial-temporal decision framework to evaluate coastal vulnerability and alternative adaptation decisions. The model framework integrates system dynamics and multicriteria analysis on the spatial scale to determine coastal vulnerability under SLR. From the building level, to cope with the increasing risk of natural hazards to coastal communities, the evaluation of adaptation strategies also requires public authorities to apply risk-based approaches, which includes uncertainties, likelihoods, and life-cycle cost-benefits (LCCB) of adaptation strategies in flood risk management (S. Dong, Yu, Farahmand, & Mostafavi, 2020; Lawrence et al., 2018; Willows, Reynard, Meadowcroft, & Connell, 2003). Yohe, Knee, and Kirshen (2011) emphasized the criticality of specifying a baseline in evaluating adaptation strategies using probability-based model framework. Haghightafshar et al. (2020) encouraged a shift from the engineering design of flood adaptation toward a risk-based adaptation design by examining recurrence intervals of flooding under non-stationarity conditions.

Risk-based adaptation decision-making to SLR must therefore be integrated into adaptation planning to inform responsibilities of different stakeholders (Hurlimann et al., 2014). Social vulnerability has been found to significantly influence community resilience against natural hazards (Y. Chen et al., 2021). In the US, although the Federal Emergency Management Agency (FEMA) takes an active role in improving community resilience through managing flood risk zones and provide hazard mitigation program, local communities are still facing divergent social vulnerability due to vulnerability of stakeholders in flood exposure, sensitivity, and adaptive capacity (Chang et al., 2021; FEMA, 2021). To incorporate social vulnerability in adaptation planning, Nguyen et al. (2019) presented a retrofitting framework for urban drainage systems based on the motivation and ability of stakeholders. Nevertheless, the framework lacks CBA components to access the financial performance of retrofitting projects. A building-level LCCB model considering social vulnerability in coastal communities could identify vulnerability in cities and improve adaptation planning. Xian, Lin, and Hatzikyriakou (2015) evaluated the flooding vulnerability of coastal buildings through a quantitative assessment of storm surge damages after Hurricane Sandy, where structure damages of properties were estimated based on a combination of cadastral parcel data and field survey data. de Ruig, Haer, de Moel, Botzen, and Aerts (2019) also applied CBA to measure benefits of adaptive measures in coastal areas of California. Zarekarizi, Srikrishnan, and Keller (2020) evaluated house elevation strategy by incorporating uncertainties of flood damage, discount rates on future flood damages. Despite increasing risk-based analysis on the building adaptation, few studies have been conducted on the city level to evaluate large-scale building adaptation planning under climate uncertainties. One of the reasons is because high computational burden in the model evaluation. Therefore, we developed a cloud-based flood adaptation model to tackle building-level adaptation challenges in coastal cities by integrating the life-cycle building damages and adaptation costs, stochastic storm surge events, and SLR projections to inform adaptation policies.

Table 1
Costs of adaptive measures per square feet.

Elevation	Single-Family Property	Mobile Home/ Manufactured House	Multi-family House	Non-residential Property
Elevation				
+0.6 m	22.16	27.03	27.56	41.35
+0.9 m	23.64	29.00	29.24	43.88
+1.8 m	24.88	30.64	30.64	45.98
+2.4 m	26.12	32.28	32.04	48.08
Wet flood-proofing				
+0.6 m	1.43	1.90	1.63	2.44
+0.9 m	2.97	3.93	3.36	5.05
Dry flood-proofing				
+0.6 m	5.53	6.19	5.81	6.86
+0.9 m	6.96	7.84	7.33	8.73

3. Methods

3.1. Damage of buildings from storm surges

SLR and storm surge varies between geographical regions. We applied the generalized extreme value (GEV) distribution to simulate the random storm surge heights (Lopez-Cantu, Prein, & Samaras, 2020). The cumulative function of GEV distribution applied in this study randomly generate storm surge in each year of simulation:

$$F(x; u, \sigma, \xi) = \exp \left\{ - \left[1 + \xi \left(\frac{x-u}{\sigma} \right)^{-\frac{1}{\xi}} \right] \right\} \quad (1)$$

In Equation 1, $F(x; u, \sigma, \xi)$ is the cumulative probability of a storm surge height, which can be randomly generated from a continuous uniform distribution $u(0,1)$. x represents the storm surge height, u, σ, ξ are the location, scale and shape parameters of a distribution, respectively. We also considered the nonstationary GEV distribution with a changing location parameter under SLR, where the location parameter changes based on the increase of sea-level in the simulation (Vitousek et al., 2017).

Since storm surge heights vary in different locations, we used a bathtub model proposed by the NOAA to derive inundation maps under each return period. A bathtub model, also called single-value surface model, is commonly used in tidal inundation mapping. Two variables, topography elevation and tidal inundation, are the primary variables in the bathtub model. The topography elevation data of the bathtub model usually comes from a DEM of the study area and the tidal inundation data could be derived from a hydrological model. In our model, we applied the local DEM data and inundation maps from NOAA’s Sea, Lake, and Overland Surges from Hurricanes (SLOSH) model to map flood inundations. To identify disconnected areas in floodplains, buildings in low laying areas that do not have hydrological connection to the flooding source are identified by overlaying flood map with local DEM data (Ghanbari, Arabi, & Obeyseker, 2020). We then adjusted building flood inundation heights under each return period based on the local flood inundation height.

The estimation of flood loss is measured similar to the flood depth-damage table in the HAZUS-MH model (Scawthorn et al., 2006). We estimated flooding damage based on the property value and inundation height (Karamouz, Fereshtehpour, Ahmadvand, & Zahmatkesh, 2016). The flood risk is estimated according to a building’s expected annual damage (EAD) in Equation (2).

$$EAD = \int_{i=0}^1 D(p_i) dp_i = \frac{1}{2} \sum_{i=1}^n (p_i - p_{i+1})(D(p_i) + D(p_{i+1})) \quad (2)$$

where $D(p_i)$ is the flood damage occurs with probability p_i , dp_i is the probability density of the hurricane event i . We employed numerical

integration method to estimate flood damage across all return periods (Olsen, Zhou, Linde, & Arnbjerg-Nielsen, 2015).

3.2. Life cycle cost and benefit analysis

A dynamic life-cycle cost and benefit (LCCB) approach for individual buildings was applied in this study to evaluate risk mitigation measures (Han & Mozumder, 2021). Three main types of adaptive measures are considered in the analysis. They are house elevation, wet-proofing, and dry-proofing. According to FEMA’s retrofitting manual, floodproofing measures are effective when flood height is lower than 1m and house elevation is usually considered when the elevating height is lower than 2.9m (FEMA, 2017). In our study, we evaluated floodproofing measures at 0.6m and 0.9m, and house elevation at 0.6m, 0.9m, 1.8m, and 2.4m, respectively. Table 1 shows unit cost information of these adaptation measures (Aerts, 2018; Burrus, Dumas, & Graham, 2001). In our sensitivity analysis, we also considered cost uncertainties of adaptive measures by assuming normal distribution of unit cost with a 0.5 coefficient of variation for each adaptive measure (Han & Mozumder, 2021; Zarkarizi et al., 2020).

We estimated initial cost for each kind of adaptive measure and assumed all implemented adaptation measures are well-maintained and effective during the simulation. Maintenance and repair costs are other sources of adaptation costs. We assumed a 5% and 3% annual maintenance and repair cost in the LCCB for floodproofing and building elevation measures, respectively (Aerts, 2018). To estimate annual flood damage cost, we adapted the damage curves from Lasage et al. (2014) to estimate the average flood damages for each adaptive measure using Equation (2). We incorporated the low SLR projection based on a historical SLR rate and chose a long analysis period $T = 100$ years in the LCCB model (Pachauri et al., 2014). Adaptation decisions will be evaluated every 10 years based on the projected SLR and discounting factors. To compare cost cash flows at different time periods during the life-cycle of the implementation of adaptive measures, a discount rate d , with mean 0.4 and standard deviation 0.2, was used to discount adaptation costs at different periods during the simulation. We did not consider the net present value of future risk in the analysis.

3.3. Adaptation scenario design

We developed four scenarios in the adaptation analysis. In adaptation scenario 1, adaptive measures of buildings are evaluated based on the LCCB method. All adaptation costs are discounted to the present value. No public adaptation is considered in the evaluation. Adaptation scenario 2 considers social vulnerability of property owners based on a derived willingness-to-pay for flood adaptive measures. In scenario 2, when the willingness-to-pay for a residential building is smaller than the discounted annual cost of an adaptive measure, the adaptive measure will not be considered in the evaluation. The evaluation of available alternative adaptive measures still relies on the LCCB. Results from adaptation scenario 2 can indicate social vulnerability in adaptation. Based on the LCCB model with social vulnerability, we designed adaptation scenario 3 and 4 by considering public adaptation using seawall and the enforced adaptation policy within flood zones. Scenario 3 estimated the height of public seawall based on the lower bound of the 95% confidence interval of the GEV distribution. In scenario 4, the seawall height is estimated based on the upper bound of the 95% confidence interval of the GEV distribution. In both scenario 3 and 4, buildings located within the 100-year flood inundation zones are required to be elevated above 1-foot of the 100-year flood inundation (Han, Ash, Mao, & Peng, 2020). However, in the last two adaptation scenarios, adaptation evaluation models outside flood zones are consistent with adaptation scenario 2.

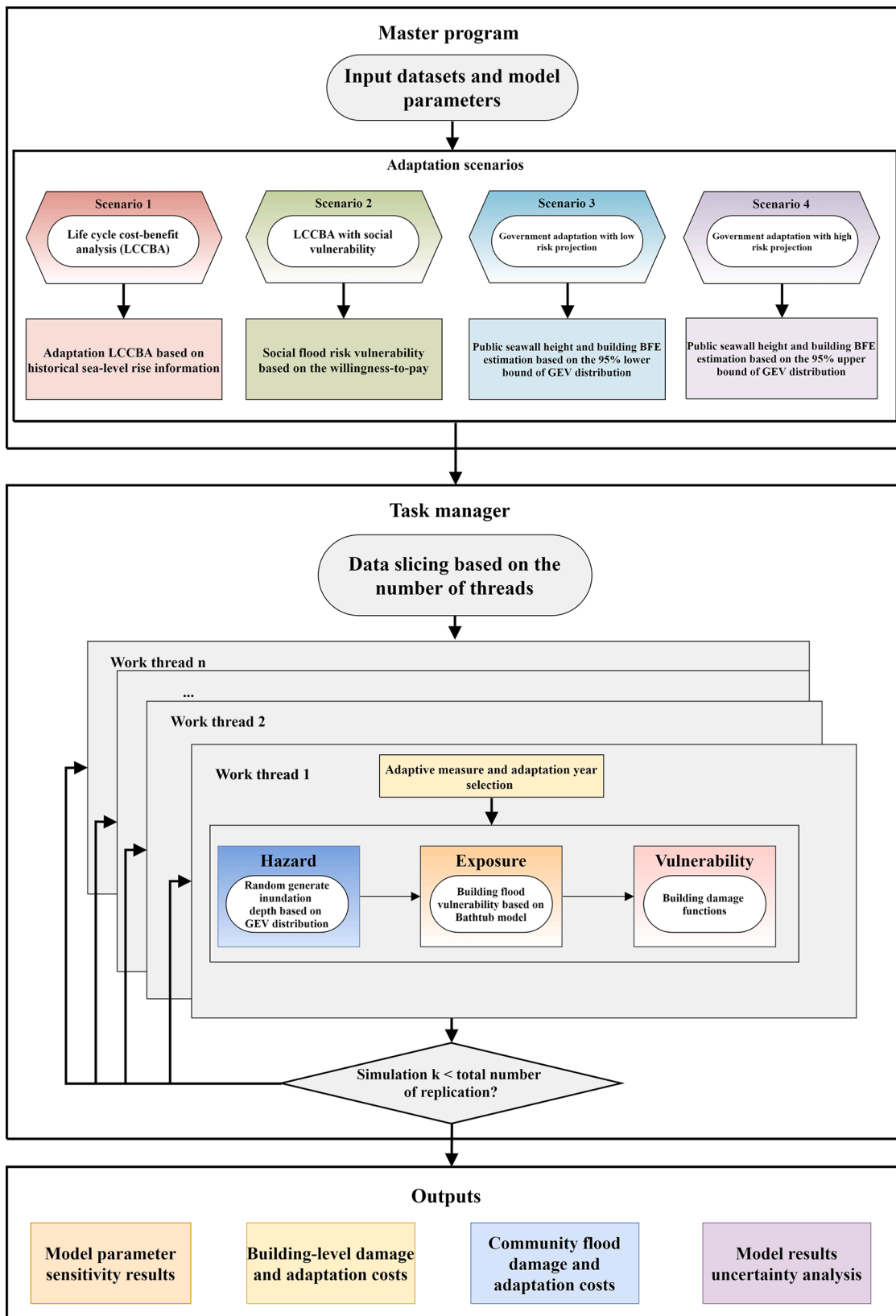


Fig. 1. A cloud-based methodology framework for adaptation evaluation with multiple parallel working threads.

3.4. The cloud-based model framework

Due to dynamic and uncertain climate conditions, the quantitative assessment of the flood exposure and the vulnerability of all buildings in

cities is a challenging task. To address time-consuming issue in the sensitivity and uncertainty analysis, we implemented a time-efficient cloud-based model framework using methods explained in above sections. To fully utilize the cloud computing resources, the model

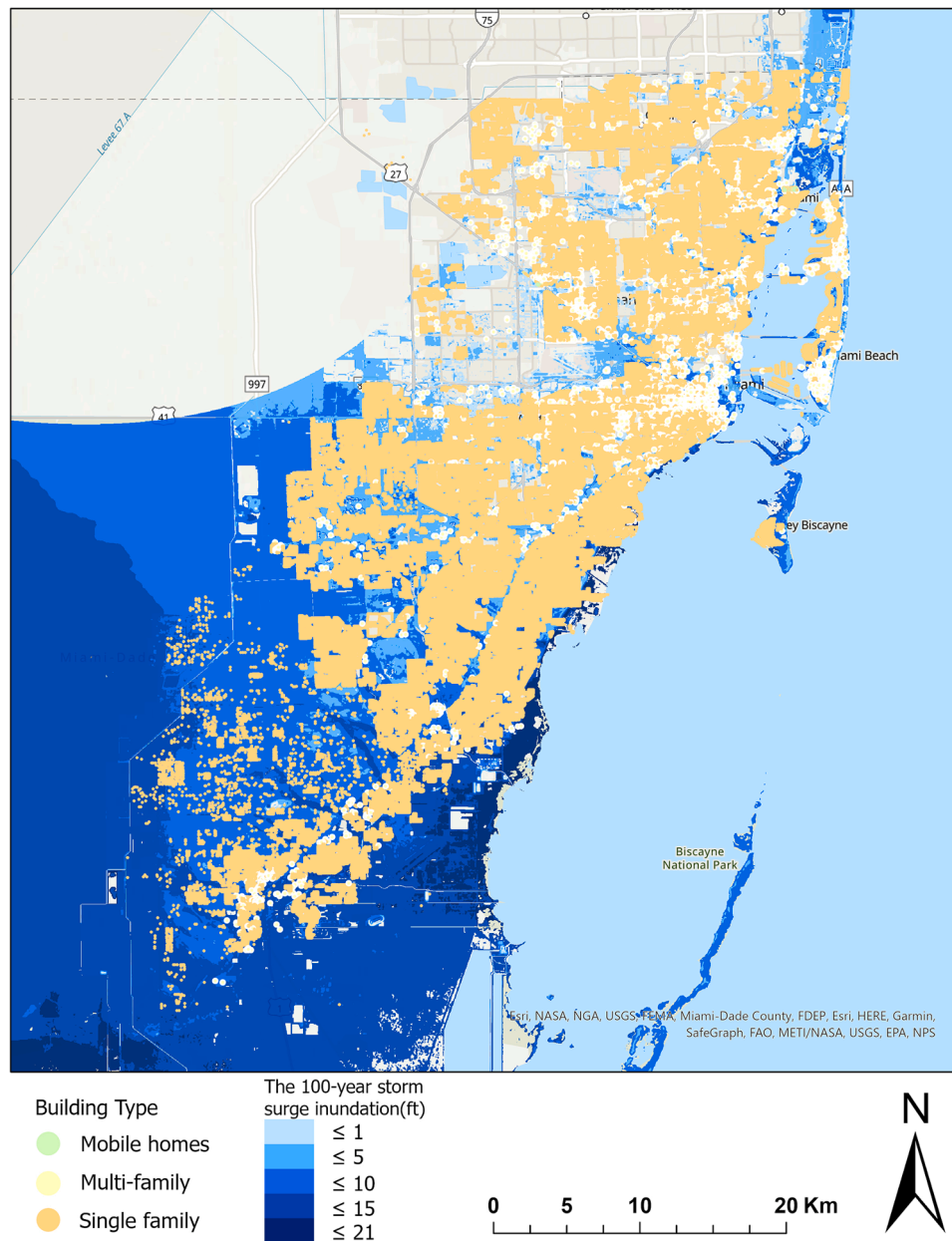


Fig. 2. Flood inundation of buildings in Miami-Dade County under the 100-year storm surge flood.

framework was implemented with multiple threads using Java and the project was built with maven. Our code can be accessed on GitHub(<https://github.com/yuh2017/MiamiFloodAdaptation.git>).

Fig. 1 shows the proposed methodology flowchart in the study. The simulation model is controlled by a master program with multiple adaptation scenarios and model parameters. Each scenario begins by executing the task manager program which contains multiple parallel working threads. The task manager will partition data into multiple sub-datasets with the same size. Afterward, each sub-dataset will be executed by a working thread independently.

In each working thread, a Monte-Carlo approach is applied to select adaptive measures and adaptation time, simulate stochastic flood hazards using the GEV distribution, evaluate building exposure based on the bathtub model, and estimate building vulnerability using the flood damage functions. Three sources of uncertainty information are included into the model evaluation, which are the uncertainty of unit costs of adaptive measures, the uncertainty of GEV distribution parameters, and the uncertainty of discount factor. We measured the hazards,

exposure, and vulnerability of all buildings for the whole simulation period on an annual basis by considering SLR. After the number of model replications reaches the predefined total simulation number (N), the community total damage, adaptation costs, and flood damage and cost information will be generated into outputs. The simulation will terminate when all working threads write their simulation results into outputs.

4. Case study area

To illustrate the methodology proposed above, we chose Miami-Dade County, Florida as the case study area in the evaluation of adaptation decisions. Miami-Dade County is one of the most vulnerable cities in the U.S. Gulf Coast region (Chang et al., 2021). We collected four kinds of geographical dataset from the US census and Florida Geographical Data Library (FGDL): the US Census and spatial data of Miami-Dade County, the cadastral parcel data, 5-m DEM data, and numerical inundation simulation data from the NOAA's SLOSH model

Table 2
Total number of properties for each type.

Property Type	Single Family	Multi-family/Condo	Public/Commercial
Count	37196	38620	925
Percentage	48.47%	50.32%	1.20%

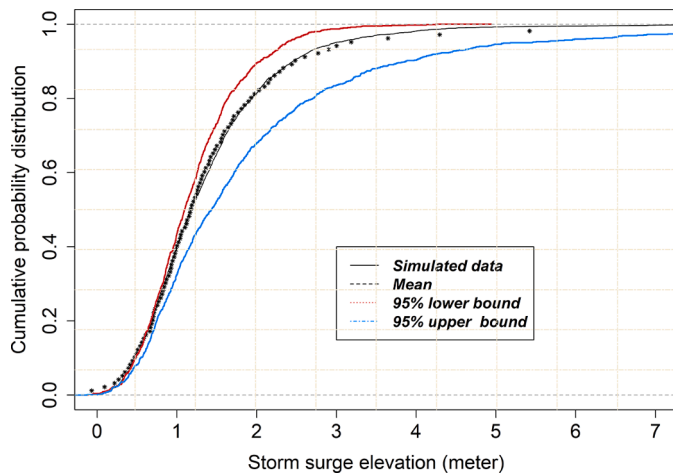


Fig. 3. The fitted cumulative distribution and 95% confidence bounds of storm surge inundation.

(Glahn, Taylor, Kurkowski, & Shaffer, 2009).

We selected buildings within the 95% of the empirical cumulative distribution of building values in Miami-Dade area. Since mobile homes takes less than 0.5% of residential buildings in Miami-Dade County, we excluded mobile homes in the evaluation. As a result, we classified three types of buildings in the analysis, including single-family houses, multi-family/condominium buildings, and public/commercial buildings. Fig. 2 shows the location of the study area and flood inundations from the 100-year storm surge in Miami-Dade County. It can be seen that most of buildings are extremely vulnerable to the 100-year storm surge. Since we only had free access up to 16 CPU cores in our cloud system, to evaluate model results in a time-efficient manner, we randomly chose 10% of buildings in the study area to illustrate the performance of our developed model. Table 2 shows the number and percentage of properties in each type. The single-family and multi-family/condominium take 48.47% and 50.32% of all buildings, respectively. Nevertheless, only about 1.2% public/commercial buildings are included in this evaluation. We fitted the cumulative distribution of flood inundation in Miami-Dade County using the local storm surge models together with the 95% upper and lower bounds in Miami-Dade County (NOAA, 2013), as shown in Fig. 3.

In adaptation scenario 2, based on a local flood risk awareness survey data (Halim, Jiang, Khan, Meng, & Mozumder, 2021), we also derived a willingness-to-pay for each residential building in Miami-Dade using a building’s type, area, value, and property owner’s income level. The linear model fitted using the stepwise linear regression is as follows:

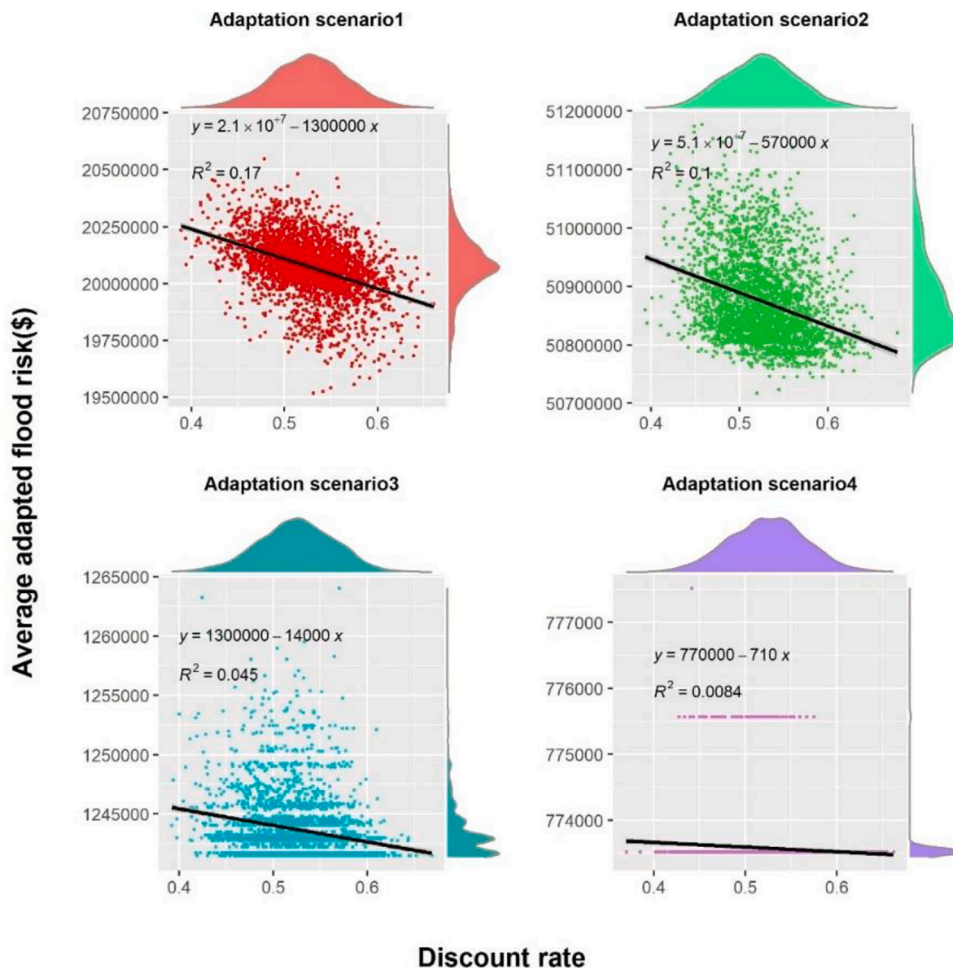


Fig. 4. Average total community flood risk reduction under changing discount rates.

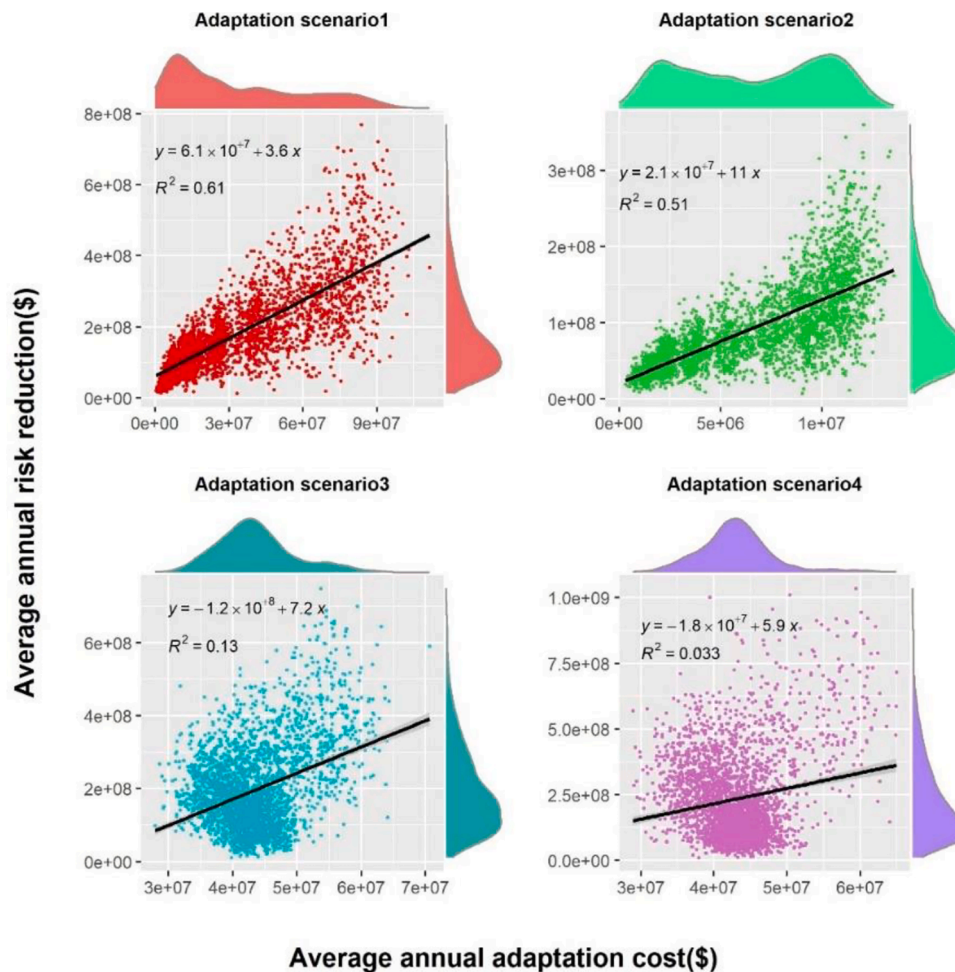


Fig. 5. Average annual community flood risk reduction with changing adaptive measure costs.

$$Pay_i = 3.102e^{-2} - 4.566e^{-3}Type_i + 2.989e^{-6} Area_i + 7.153e^{-9} Value_i - 3.165e^{-3} Income_i \tag{3}$$

In Equation (3), the Pay_i represents the average value of willingness-to-pay of the property owner in building i , $Type_i$ is the type of the residential building, $Area_i$ presents the area of building i in square feet, and the $Value_i$ is the listed value for building i , $Income_i$ is a randomly generated income in for the property owner of building i . We randomly generated the income of property owner based on their self-reported income level and property value. In adaptation scenario 3, we estimated a 2-ft public seawall based on the LCCB model using the lower bound of the 95% confidence interval of the GEV distribution in Fig. 3. In adaptation scenario 4, a 6ft public seawall was estimated based on the upper bound of the 95% confidence interval of the GEV distribution.

5. Results

We evaluated adaptive measures and simulated storm surge heights by randomly generating the GEV distribution parameters in each year of the simulation using 16 CPU cores in the cloud computing system. We then employed the low SLR rate to represent the future SLR projection by comparing historical mean sea-level rise in the county (NOAA, 2013). Results are then aggregated based on 3000 model replications with convergence calculation (Han & Mozumder, 2021).

5.1. Model sensitivity

To evaluate model sensitivity, we utilized both local and global sensitivity analysis (Saltelli & Annoni, 2010). Since other sources of uncertainties may affect sensitivity results of the discount factor in the global sensitivity analysis, a local sensitivity analysis was conducted by randomly generating discount rates while keeping other variables constant. Instead, a global sensitivity analysis was applied for costs of adaptive measures. We randomly changed all model parameters based on their assumed distributions. These parameters include the discount factor, parameters for the GEV distributions, and the unit costs for adaptive measures. Sensitivity results were displayed in scatter plots and marginal distributions. In Fig. 4, each point represents the adapted community flood risk reduction measures at the end of each simulation under a discount factor. We fitted a linear model to examine effects of discount factors on adaptation outcomes. We found that a higher discount factor could decrease community flood risk reduction measures in adaptation scenario 1. This result was obtained based on the assumption that future flood risk reduction measures were not discounted in the LCCB model. Due to higher present value of adaptation under higher discount factors, a high discount factor will result in more adaptation activities during the early stage of model simulations. Because of social

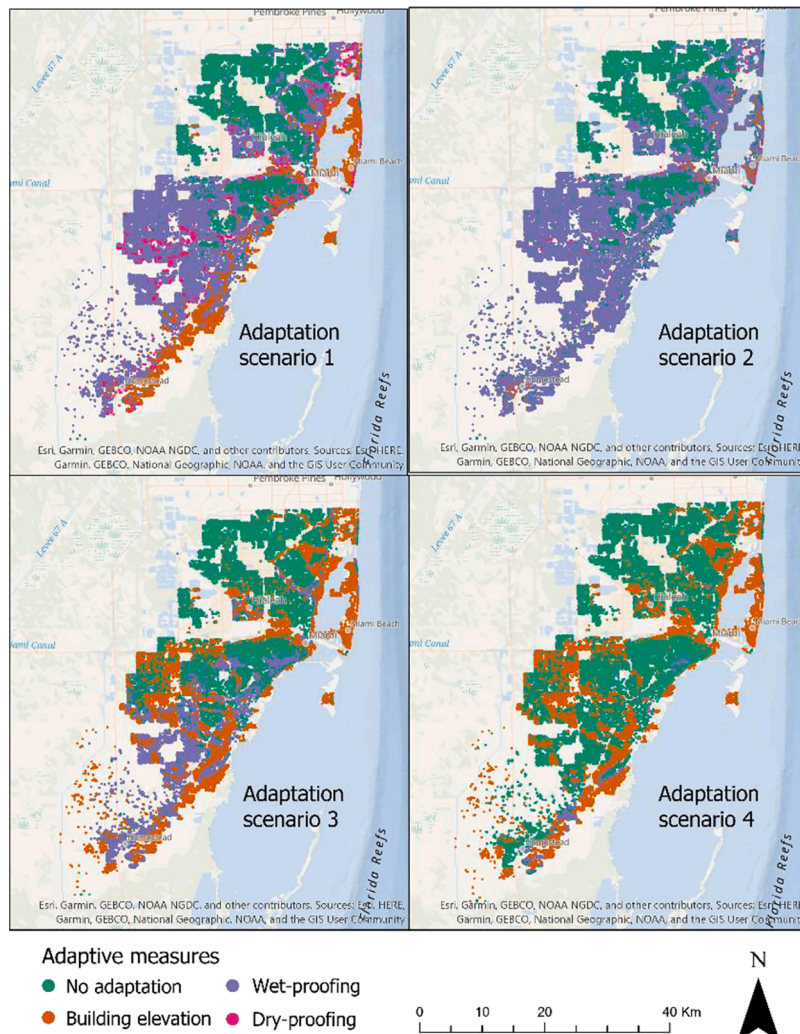


Fig. 6. Proposed adaptive measures under the low SLR projection.

vulnerability of property owners in scenario 2, the effect of discount factor on community flood risk reduction measures is more random. Since adaptation scenario 3 and 4 considers public seawall and enforced risk mitigation requirement within the flood zone, the non-linear relationship between discount factor and community flood risk reduction is significant. In scenario 4, the average adapted flood risk reduction measures in the county varies little with the discount factor. Fig. 5 then shows the sensitivity of community adaptation costs on community's average annual risk reduction. The average annual risk reduction was calculated as the differences between the community flood risk without considering adaptation and the community flood risk considering adaptation. On average, higher adaptation cost will produce higher total risk reduction in the community. However, in adaptation scenario 3 and 4, effects of adaptation cost on community risk reduction are non-linear due to public adaptation.

5.2. Adaptation scenario results

We showed that the adaptive measures in Miami-Dade County for four adaptation scenarios in Fig. 6. In general, areas in the central, north and northeast of the county have higher elevation, thus buildings have lower risk. Therefore, fewer buildings in these areas were implemented with adaptive measures in all scenarios. In adaptation scenario 1, most buildings near the coastline, such as areas around Miami Beach and southwest part of the county, were implemented with building elevation

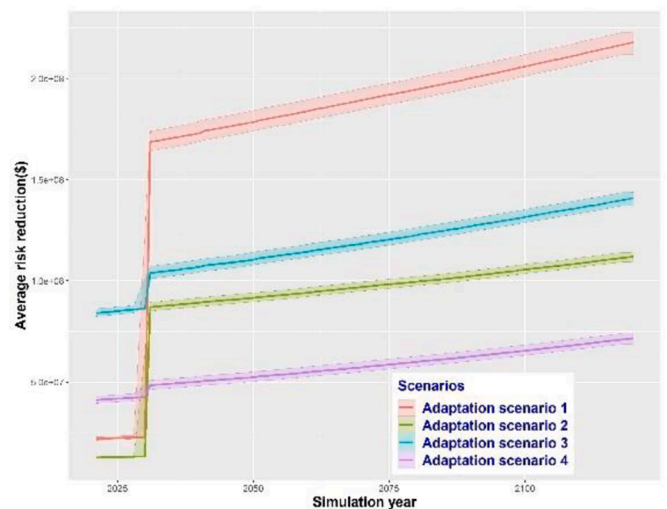


Fig. 7. The averaged risk reductions by private adaptive measures of buildings under the SLR projection.

due to higher flood risk in these areas. However, only a small number of buildings near the coastline, such as Miami Beach area, were implemented with building elevation measure. Most buildings in floodplains

Table 3
The average adaptation outcomes for each type of building.

Building Type	Flood damage without adaptation (\$)	Adapted flood damage (\$)	Discounted annual adaptation cost (\$)	Benefit to cost ratio
Adaptation scenario 1				
Single-family	4134	2253	335	5.62
Multi-family/Condo	3676	1889	155	11.52
Public/Commercial	4339	2327	126	16.00
Adaptation scenario 2				
Single-family	4134	3311	79	10.39
Multi-family/Condo	3676	2766	52	17.65
Public/Commercial	4339	2813	61	24.94
Adaptation scenario 3				
Single-family	4134	1554	673	3.83
Multi-family/Condo	3676	1351	317	7.33
Public/Commercial	4339	1570	248	11.17
Adaptation scenario 4				
Single-family	4134	901	662	4.88
Multi-family/Condo	3676	880	330	8.47
Public/Commercial	4339	885	288	11.97

were implemented with wet-proofing. This result indicates that the cost of building elevation could be a crucial factor that limits its adoption. Buildings in southeast part have relatively lower risk, and therefore, wet-proofing is a more cost-effective measure in reducing flood risk of buildings. In adaptation scenario 1, a small percentage of buildings near water and river canals were implemented with dry-proofing. However, only a few buildings in scenario 2 were implemented with dry-proofing.

This result shows that dry-proofing is less cost effective compared with building elevation and wet-proofing on average.

A significant number of buildings in adaptation scenario 3 and 4 were implemented with building elevation. This is because most of these buildings are located in the 100-year flood zone, and therefore, needs to be elevated to 1-foot above the 100-year flood height. Moreover, scenario 3 has more buildings implemented with wet-proofing in the south

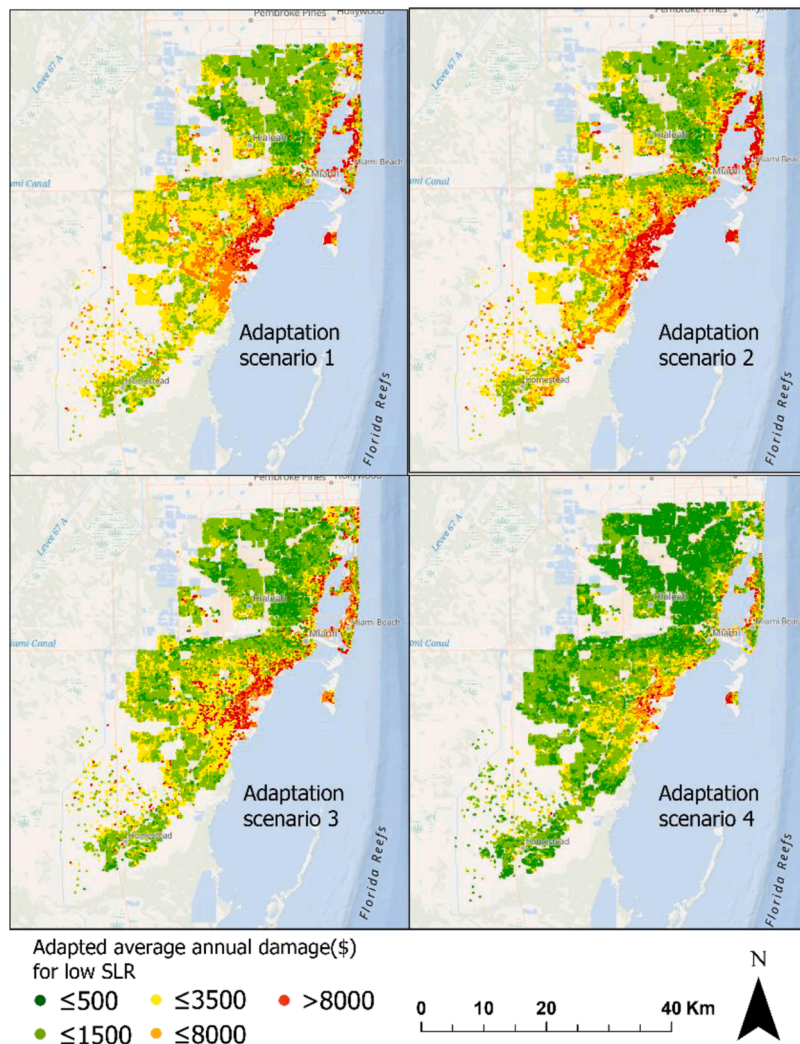


Fig. 8. The average annual damages of buildings under the low SLR projection.

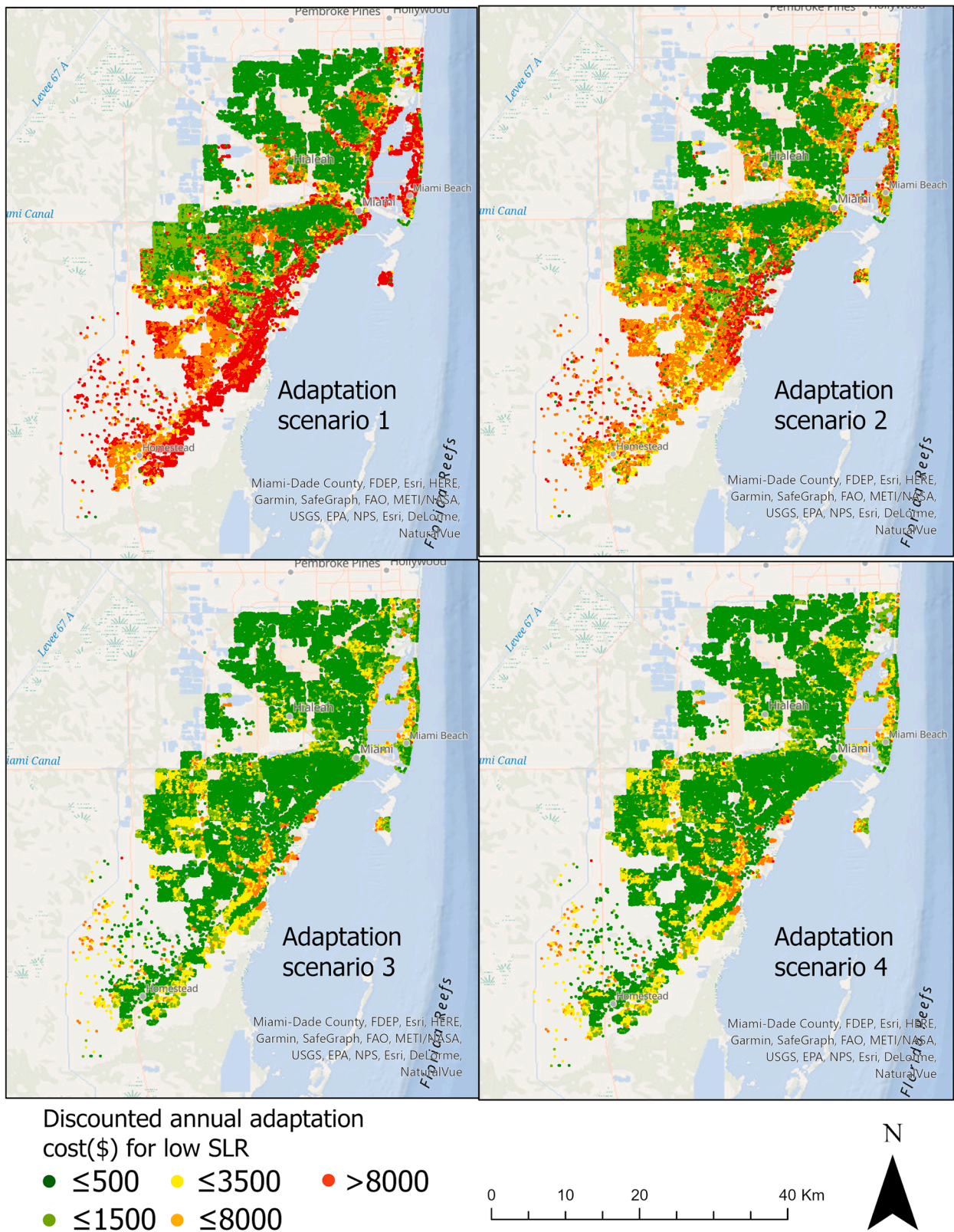


Fig. 9. The discounted average annual adaptation costs of buildings under the low SLR projection.

side of the county. This indicates that flood risk in scenario 3 could still cause damages to buildings in these areas even under the low SLR projection, and meanwhile, wet-proofing measures are more cost effective in reducing risk in these areas.

Fig. 7 shows the average community risk reduction of adaptive

measures with 95% confidence intervals in each adaptation scenario. The total average community risk reduction could indicate the effectiveness of adaptive measures in reducing flood risk under each adaptation strategy. On average, risk reductions are increasing given the increasing number of community adaptive measures. Risk reductions in

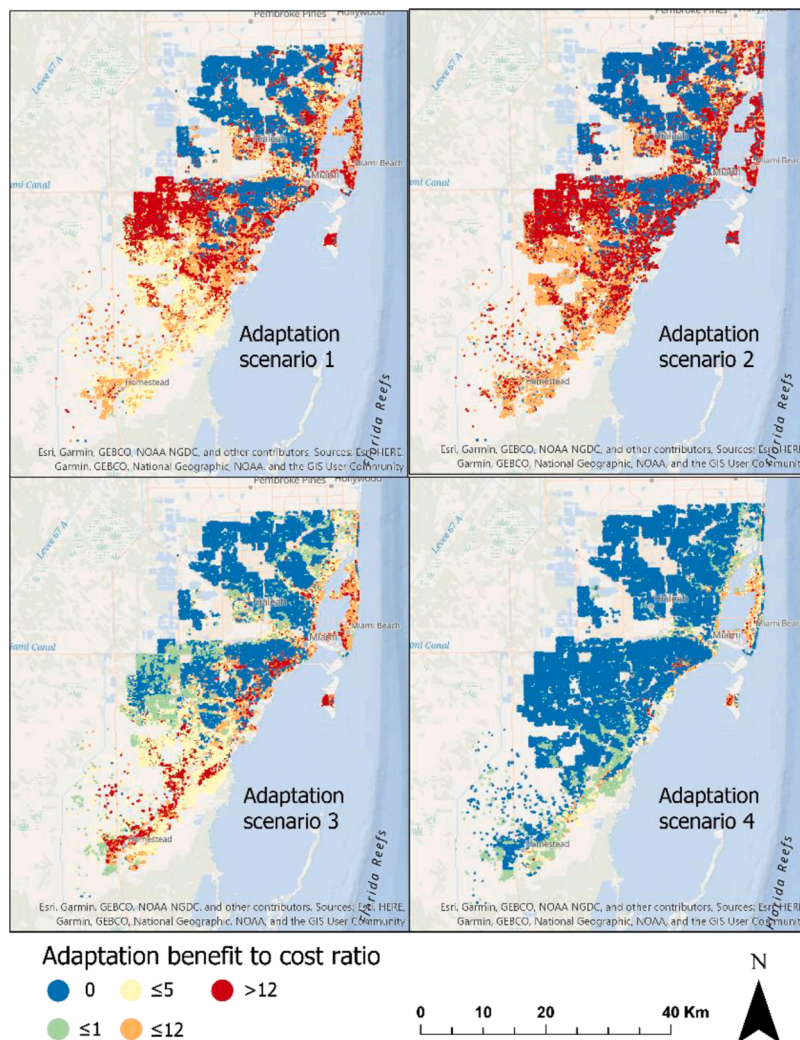


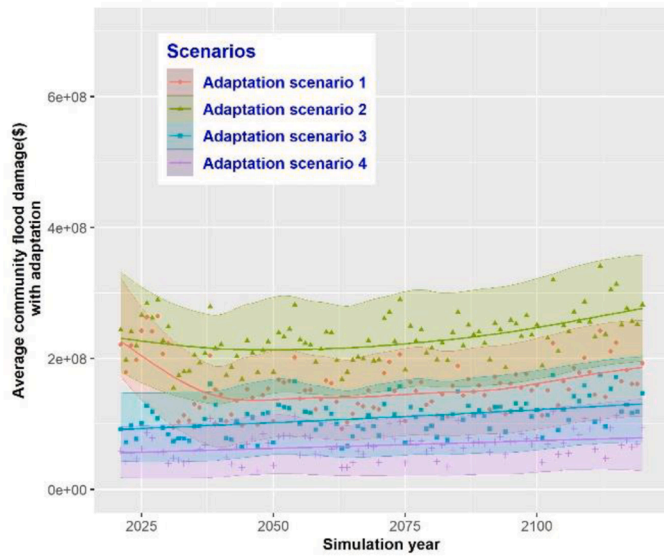
Fig. 10. The average benefit to cost ratios of buildings under the low SLR projection.

all scenarios increased significantly after 2030 because most adaptive measures are planned to be implemented in 2030. This simulation result indicates that highly vulnerable buildings in Miami-Dade County need to be protected at the early stage. Afterward, as more adaptive measures are implemented, the averaged total community risk reductions under all adaptation scenarios increase smoothly. Adaptation scenario 1 has much higher risk reductions compared to other adaptation scenarios. Scenario 3 has the second highest risk reduction due to the enforced building elevations in the flood zone. Due to the installation of a 6ft public seawall in adaptation scenario 4, risk reduction by private adaptive measures in adaptation scenario 2 is even higher than adaptation scenario 4.

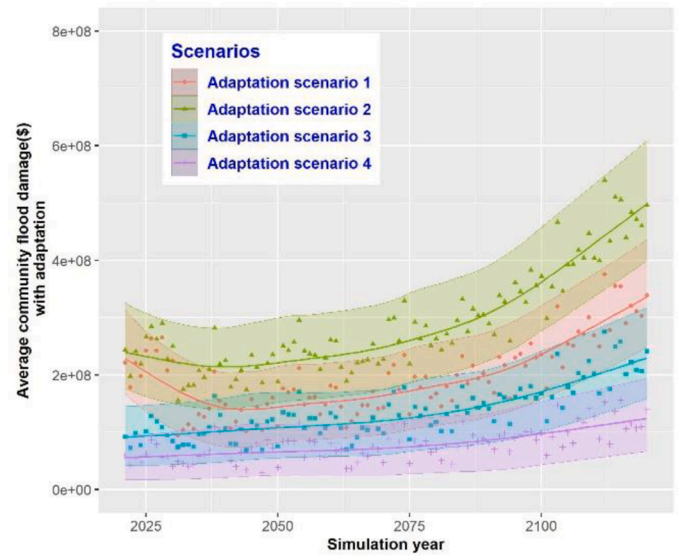
Table 3 shows flood damages, the discounted annual adaptation cost, and benefit to cost ratios for each type of building that has an implemented adaptive measure. Flood damages without adaptation are the same for each adaptation scenario. When considering adaptation, single-family building has the highest adapted average flood damage and discounted annual adaptation costs. The public/commercial buildings have the highest benefit to cost ratios. Adaptation scenario 3 and 4 have adapted flood damages ranging between \$880 and \$1554, which are significantly smaller than results in adaptation scenario 1 and 2. As for buildings, the multi-family/condo has the lowest annual adaptation costs. This implies that multi-family/condo buildings have lower life cycle costs in adaptation. Most multi-family/condo buildings with an adaptive measure were implemented with wet-proofing. The reason

could be that multi-family/condo buildings have relatively lower flood risk or building elevation cost is too high for multi-family/condo buildings.

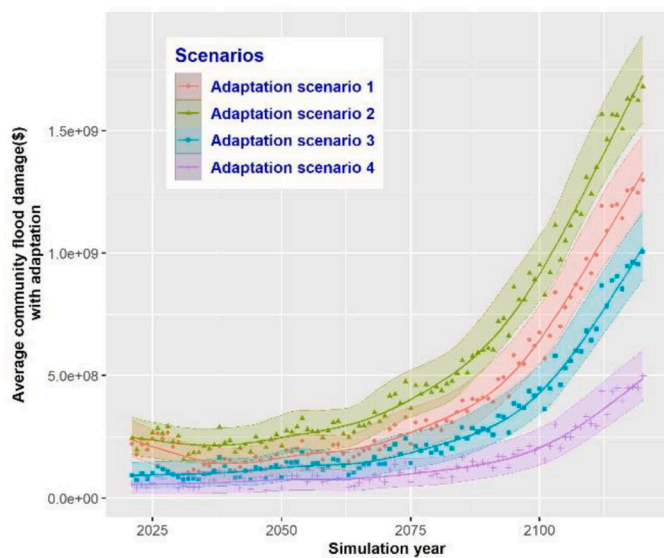
To identify the vulnerability of buildings, we examined the average flood damage of buildings and adaptation costs under four adaptation scenarios. Results are shown in Fig. 8-10. Fig. 8 shows spatial distribution of the adapted average annual damage of buildings under the low SLR projection. On average, since the implementation of public seawall in adaptation scenario 3 and 4, the adapted building damages in these two scenarios are lower compared to results in scenario 1 and 2. In scenario 2, property owners with lower willingness-to-pay will invest less on adaptive measures. Therefore, it has more adapted building damages compared to scenario 1. In adaptation scenario 1, Miami Beach area and east coastal of the county have high flood damage even with adaptive measures. The south and west parts of the county show moderate flood damages. In adaptation scenario 2, almost all buildings near the east coast of the county have high flood damages. The number of vulnerable buildings increased substantially compare to adaptation scenario 1. Adaptation scenario 3 has several areas with high flood damages, which are located in central east of the county and Miami Beach. Benefit from a 2ft public seawall and enforced adaptation policy within flood zones, large number of buildings in the south of the county substantially mitigated their flood risk. Compared to scenario 2, these areas have high social vulnerability. Moreover, buildings that are near the shoreline and outside of the 100-year flood zones are more



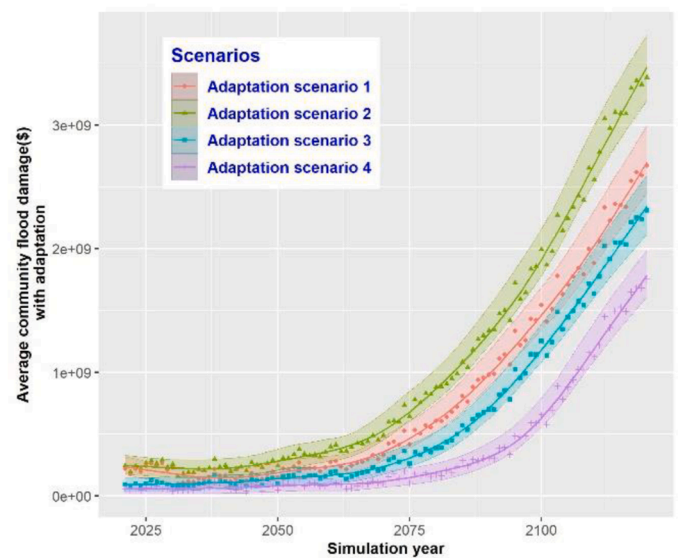
(a) Low SLR



(b) Intermediate low SLR



(c) Intermediate high SLR



(d) High SLR

Fig. 11. Total community flood damage under SLR projections.

vulnerable in scenario 2. Adaptation scenario 4 have the lowest flood damage across the county. Compared to adaptation scenario 3, only a small number of buildings in central east of the county and Miami Beach are highly vulnerable due to their exposure to storm surges.

Fig. 9 shows discounted annual cost for building adaptive measures under the low SLR scenario. It can be seen that adaptation scenario 1 has higher average annual adaptation costs compared to other adaptation scenarios. Coastal areas and the southeast of the county in scenario 1 have the highest adaptation costs. Although the discounted annual adaptation costs in scenario 2 are relatively higher within the 100-year flood zone, costs in these areas are much lower compared to scenario 1. Adaptation costs in scenario 3 and 4 are very close and are both lower than \$8000 in vulnerable areas due to the protection of public seawalls. To further investigate adaptation benefits of building adaptation, Fig. 10

shows the average benefits to cost ratios in each adaptation scenario. When the benefit to cost ratio equals 0, it means no adaptation was considered in the evaluation. Areas in the south, central west, and east coastal areas of the county have high benefit to cost ratios on average in both scenario 1 and 2, while scenario 2 has the highest adaptation benefits to cost ratios on average. Although the central west of the county has relatively lower risk compared to coastal areas, this region has a high benefit to cost ratios for buildings. It could be the reason that the implementation of low cost measures, such as wet-proofing, in these areas has high flood risk reduction. Compare to adaptation scenario 4, adaptation scenario 3 has higher benefit to cost ratios in the flood zone, but also has benefit to cost ratios lower than 1 in areas with low flood risk. This indicates that the average risk reduction could be lower than the discounted annual costs in these areas.

5.3. Impacts of uncertain SLR

To incorporate impacts of uncertain SLR on community flood risk, we further simulated the average adapted flood damage under four SLR scenarios. These four SLR scenarios are based on NOAA's low, intermediate low, intermediate high, and high SLR projections (W. V. Sweet et al., 2017). The four SLR scenarios assume a 0.2m, 0.5m, 1.2m, and 2.0m SLR after 100 years projection. In our simulation, we randomly generated storm surge heights by considering the rising sea-level height. Fig. 11 shows community adaptation damage under the four adaptation scenarios and SLR scenarios. Due to the low frequency nature of flood appearance, the scatter plots of average community damages fluctuate within a range. Therefore, we fitted the mean community damage and 95% confidence intervals using the averaged community damage after 1000 model replications. Adaptation scenario 1 initially has a close average community damage with adaptation scenario 2, but the damage decreases substantially after 2035 due to more implemented adaptive measures before that time. The average community damage in adaptation scenario 1 ranges from \$221 million to \$2750 million under all SLR projections. Adaptation scenario 2 has higher community damage compared to other adaptation scenarios, where the community average damage ranges from \$244 million to \$3440 million. This result reflects social vulnerability in adaptation scenario 2 and no public adaptation or enforced adaptation policies was considered in the flood zones. Under the low SLR scenario, the community damages in the four adaptation scenarios are close and have large overlaps between each other. However, as SLR rates increasing, the average community damages in adaptation scenario 1 and 2 increase more significantly compared to those in adaptation scenario 3 and 4. When SLR projections are low, community damages in adaptation scenario 3 are relatively slow, ranging between \$92 million and \$175 million. However, when SLR rates are high, community damages in adaptation scenario 3 are close to those in adaptation scenario 1. At the end of simulation in the high SLR projection, community damages in adaptation scenario 3 is about \$2390 million. Adaptation scenario 4 has the lowest adapted community damage under all SLR projections, where community average damages range from \$59.3 million to \$1820 million. These results imply that, compared to other adaptation scenarios, the public seawall based on the upper bound of GEV distribution is more effective in protecting the community from increasing threats of uncertain SLR.

6. Discussions and Conclusions

This study developed a risk-based adaptation assessment framework to facilitate community flood risk management on the building-level using cloud computing. We integrated four adaptation scenarios to illustrate how flood adaptation strategies could improve community resilience under SLR. Our model results considered adaptation outcomes under stochastic flood appearance in adaptation decision-making. Results illustrated the long-term benefits of flood adaptation on the spatial and temporal scales, as well as uncertainties of discount factor and adaptive measure costs in Miami-Dade County, FL. Due to social vulnerability of individual property owners, the adaptation outcome considering social vulnerability was less effective in mitigating community flood risk under SLR. Instead, a LCCB adaptation framework could be more effective in improving building resilience. Nevertheless, the LCCB adaptation model performed less than adaptation models with public seawall protection and enforced adaptation policy within flood zones. This conclusion indicates that effective community flood risk mitigation needs to go beyond CBA and integrate enforced public adaptation policies in vulnerable locations.

Although the developed model in this research could be applied to examine building damages from storm surge in coastal communities under SLR. There are limitations to this study. First, this study uses a bathtub model to evaluate inundations of storm surge heights. The bathtub model is a passive flood mapping approach which does not

consider local topography, bathymetry, and wave exposure of the study area. Anderson et al. (2018) found that a bathtub model could underestimate local flood inundations at high tide in Hawaii. Future studies could integrate the developed model in this study with hydrological models to more accurately measure flood inundations and adaptation benefits on the spatial scale (Criado, Martínez-Graña, San Román, & Santos-Francés, 2019). Second, this study uses seawall as the public adaptation measure because it is more straightforward to quantify costs and benefits of hard adaptation measures. Compare to hard adaptation infrastructures, natural-based adaptation solutions are more appealing due to they have lower cost and potential ecological and environmental benefits (Kabisch, Korn, Stadler, & Bonn, 2017). Future studies could further investigate effects of natural-based adaptation measures, such as wetland, on improving coastal resilience. Third, the four adaptation scenarios are based on the LCCB method. Although the LCCB model could capture the life cycle costs and benefits of building adaptation in the decision-making, the cascading costs of climate disasters, such as interdependent socioeconomic costs, could not be captured in the simulation (Najafi et al., 2021). To better evaluate indirect benefits of adaptation, future studies could either incorporate an input-output model or a computational generalized equation model into the current adaptation model (Zhang & Peeta, 2011). Nevertheless, our presented model provides a high performance risk-based simulation framework in evaluating adaptation strategies with multiple parallel working threads using cloud computing, the developed model in this study incorporates multiple sources of parameter uncertainties and could facilitate risk communications between public and private sectors in participatory planning for flood risk mitigation.

Declaration of Competing Interest

We have no conflicts of interest to disclose.

Acknowledgements

We acknowledge the support from the National Science Foundation [Award #1832693: CRISP 2.0 Type 2: Collaborative Research: Organizing Decentralized Resilience in Critical Interdependent-Infrastructure Systems and Processes (ORDER-CRISP)]. However, the authors are solely responsible for the findings in this document.

References

- Aerts, J. C. J. H. (2018). A Review of Cost Estimates for Flood Adaptation. *Water*, 10(11), 1646. <https://doi.org/10.3390/w10111646>
- Anderson, T. R., Fletcher, C. H., Barbee, M. M., Romine, B. M., Lemmo, S., & Delevaux, J. M. S. (2018). Modeling multiple sea level rise stresses reveals up to twice the land at risk compared to strictly passive flooding methods. *Scientific Reports*, 8(1), 14484. <https://doi.org/10.1038/s41598-018-32658-x>
- Buchanan, M. K., Kulp, S., Cushing, L., Morello-Frosch, R., Nedwick, T., & Strauss, B. (2020). Sea level rise and coastal flooding threaten affordable housing. *Environmental Research Letters*, 15(12), Article 124020. <https://doi.org/10.1088/1748-9326/abb266>
- Burrus, R. T., Dumas, C. F., & Graham, J. E. (2001). The cost of coastal storm surge damage reduction. *COST ENGINEERING-ANN ARBOR THEN MORGANTOWN*, 43(3), 38–44.
- Chang, H., Pallathadka, A., Sauer, J., Grimm, N. B., Zimmerman, R., Cheng, C., ... Herreros-Cantis, P. (2021). Assessment of urban flood vulnerability using the social-ecological-technological systems framework in six US cities. *Sustainable Cities and Society*, 68, Article 102786. <https://doi.org/10.1016/j.scs.2021.102786>
- Chen, W., & Zhang, L. (2021). Predicting building damages in mega-disasters under uncertainty: An improved Bayesian network learning approach. *Sustainable Cities and Society*, 66, Article 102689. <https://doi.org/10.1016/j.scs.2020.102689>
- Chen, Y., Liu, T., Ge, Y., Xia, S., Yuan, Y., Li, W., & Xu, H. (2021). Examining social vulnerability to flood of affordable housing communities in Nanjing, China: Building long-term disaster resilience of low-income communities. *Sustainable Cities and Society*, 71, Article 102939. <https://doi.org/10.1016/j.scs.2021.102939>
- Criado, M., Martínez-Graña, A., San Román, J. S., & Santos-Francés, F. (2019). Flood Risk Evaluation in Urban Spaces: The Study Case of Tormes River (Salamanca, Spain). *International Journal of Environmental Research and Public Health*, 16(1), 5. <https://doi.org/10.3390/ijerph16010005>
- Cutler, E. M., Albert, M. R., & White, K. D. (2020). Tradeoffs between beach nourishment and managed retreat: Insights from dynamic programming for climate adaptation

- decisions. *Environmental Modelling & Software*, 125, Article 104603. <https://doi.org/10.1016/j.envsoft.2019.104603>
- de Ruig, L. T., Haer, T., de Moel, H., Botzen, W. J. W., & Aerts, J. C. J. H. (2019). A micro-scale cost-benefit analysis of building-level flood risk adaptation measures in Los Angeles. *Water Resources and Economics*, Article 100147. <https://doi.org/10.1016/j.wre.2019.100147>
- Dong, S., Yu, T., Farahmand, H., & Mostafavi, A. (2020). Probabilistic modeling of cascading failure risk in interdependent channel and road networks in urban flooding. *Sustainable Cities and Society*, 62, Article 102398. <https://doi.org/10.1016/j.scs.2020.102398>
- Dong, Y., & Frangopol, D. M. (2017). Adaptation Optimization of Residential Buildings under Hurricane Threat Considering Climate Change in a Lifecycle Context. *Journal of Performance of Constructed Facilities*, 31(6), Article 04017099. [https://doi.org/10.1061/\(ASCE\)CF.1943-5509.0001088](https://doi.org/10.1061/(ASCE)CF.1943-5509.0001088)
- FEMA. (2017, 07/31/2017). Homeowner's Guide to Retrofitting. Retrieved from <https://www.fema.gov/homeowners-guide-retrofitting>.
- FEMA. (2021, February 11, 2021). Community Flood Risk Reduction. Retrieved from <https://www.fema.gov/case-study/community-flood-risk-reduction>.
- Garner, G., Reed, P., & Keller, K. (2016). Climate risk management requires explicit representation of societal trade-offs. *Climatic Change*, 134(4), 713–723. <https://doi.org/10.1007/s10584-016-1607-3>
- Ghanbari, M., Arabi, M., & Obeyseker, J. (2020). Chronic and Acute Coastal Flood Risks to Assets and Communities in Southeast Florida. *Journal of Water Resources Planning and Management*, 146(7), Article 04020049. [https://doi.org/10.1061/\(ASCE\)WR.1943-5452.0001245](https://doi.org/10.1061/(ASCE)WR.1943-5452.0001245)
- Ghanbari, M., Arabi, M., Obeyseker, J., & Sweet, W. (2019). A Coherent Statistical Model for Coastal Flood Frequency Analysis Under Nonstationary Sea Level Conditions. *Earth's Future*, 7(2), 162–177. <https://doi.org/10.1029/2018EF001089>
- Glahn, B., Taylor, A., Kurkowski, N., & Shaffer, W.A. (2009). The role of the SLOSH model in National Weather Service storm surge forecasting. 33(1), 3-14.
- Haghighatafshar, S., Becker, P., Moddemeyer, S., Persson, A., Sörensen, J., Aspegren, H., & Jönsson, K. (2020). Paradigm shift in engineering of pluvial floods: From historical recurrence intervals to risk-based design for an uncertain future. *Sustainable Cities and Society*, 61, Article 102317. <https://doi.org/10.1016/j.scs.2020.102317>
- Halim, N., Jiang, F., Khan, M., Meng, S., & Mozumder, P. (2021). Household Evacuation Planning and Preparation for Future Hurricanes: Role of Utility Service Disruptions. *Transportation Research Record*. <https://doi.org/10.1177/03611981211014529>, 03611981211014529.
- Hallegatte, S. (2009). Strategies to adapt to an uncertain climate change. *Global Environmental Change*, 19(2), 240–247. <https://doi.org/10.1016/j.gloenvcha.2008.12.003>
- Han, Y., Ash, K., Mao, L., & Peng, Z.-R. (2020). An agent-based model for community flood adaptation under uncertain sea-level rise. *Climatic Change*, 162(4), 2257–2276. <https://doi.org/10.1007/s10584-020-02802-6>
- Han, Y., & Mozumder, P. (2021). Building-level adaptation analysis under uncertain sea-level rise. *Climate Risk Management*, 32, 100305. doi:<https://doi.org/10.1016/j.crm.2021.100305>.
- Helmrich, A. M., & Chester, M. V. (2020). Reconciling complexity and deep uncertainty in infrastructure design for climate adaptation. *Sustainable and Resilient Infrastructure*, 1–17. <https://doi.org/10.1080/23789689.2019.1708179>
- Hurlimann, A., Barnett, J., Fincher, R., Osbaldiston, N., Mortreux, C., & Graham, S. (2014). Urban planning and sustainable adaptation to sea-level rise. *Landscape and Urban Planning*, 126, 84–93. <https://doi.org/10.1016/j.landurbplan.2013.12.013>
- Kabisch, N., Korn, H., Stadler, J., & Bonn, A. (2017). *Nature-based solutions to climate change adaptation in urban areas: Linkages between science, policy and practice*. Springer Nature.
- Karamouz, M., Fereshtehpour, M., Ahmadvand, F., & Zahmatkesh, Z. (2016). Coastal Flood Damage Estimator: An Alternative to FEMA's HAZUS Platform. *Journal of Irrigation and Drainage Engineering*, (6), 142. doi:[Artn 0401601610.1061/\(ASCE\)IR.1943-4774.0001017](https://doi.org/10.1061/(ASCE)IR.1943-4774.0001017).
- Lasage, R., Veldkamp, T. I. E., de Moel, H., Van, T. C., Phi, H. L., Vellinga, P., & Aerts, J. C. J. H. (2014). Assessment of the effectiveness of flood adaptation strategies for HCMC. *Natural Hazards and Earth System Sciences*, 14(6), 1441–1457. <https://doi.org/10.5194/nhess-14-1441-2014>
- Lawrence, J., Bell, R., Blackett, P., Stephens, S., Allan, S. J. E. s., & policy. (2018). National guidance for adapting to coastal hazards and sea-level rise: Anticipating change, when and how to change pathway. 82, 100-107.
- Lee, B. S., Haran, M., & Keller, K. (2017). Multidecadal Scale Detection Time for Potentially Increasing Atlantic Storm Surges in a Warming Climate. *Geophysical Research Letters*, 44(20). <https://doi.org/10.1002/2017GL074606>, 10,617-610,623.
- Lopez-Cantu, T., Prein, A. F., & Samaras, C. (2020). Uncertainties in Future U.S. Extreme Precipitation From Downscaled Climate Projections. *Geophysical Research Letters*, 47 (9). <https://doi.org/10.1029/2019GL086797>. e2019GL086797.
- Lyu, H.-M., Zhou, W.-H., Shen, S.-L., & Zhou, A.-N. (2020). Inundation risk assessment of metro system using AHP and TFN-AHP in Shenzhen. *Sustainable Cities and Society*, 56, Article 102103. <https://doi.org/10.1016/j.scs.2020.102103>
- Marangoni, G., Lamontagne, J. R., Quinn, J. D., Reed, P. M., & Keller, K. (2021). Adaptive mitigation strategies hedge against extreme climate futures. *Climatic Change*, 166(3), 37. <https://doi.org/10.1007/s10584-021-03132-x>
- Martínez-Graña, A., Gómez, D., Santos-Francés, F., Bardají, T., Goy, J. L., & Zazo, C. (2018). Analysis of Flood Risk Due to Sea Level Rise in the Menor Sea (Murcia, Spain). *Sustainability*, 10(3), 780.
- McAlpine, S. A., & Porter, J. R. (2018). Estimating Recent Local Impacts of Sea-Level Rise on Current Real-Estate Losses: A Housing Market Case Study in Miami-Dade, Florida. *Population Research and Policy Review*, 37(6), 871–895. <https://doi.org/10.1007/s11113-018-9473-5>
- Najafi, M. R., Zhang, Y., & Martyn, N. (2021). A flood risk assessment framework for interdependent infrastructure systems in coastal environments. *Sustainable Cities and Society*, 64, Article 102516. <https://doi.org/10.1016/j.scs.2020.102516>
- NCEI. (2021). *U.S. Billion-Dollar Weather and Climate Disasters*. Retrieved from <https://www.ncdc.noaa.gov/billions/>.
- Nguyen, H. Q., Radhakrishnan, M., Bui, T. K. N., Tran, D. D., Ho, L. P., Tong, V. T., ... Ho, H. L. (2019). Evaluation of retrofitting responses to urban flood risk in Ho Chi Minh City using the Motivation and Ability (MOTA) framework. *Sustainable Cities and Society*, 47, Article 101465. <https://doi.org/10.1016/j.scs.2019.101465>
- NOAA. (2010). *Mapping Inundation Uncertainty*. Retrieved from.
- NOAA. (2013). *Extreme water levels of the United States 1893-2010* (NOAA Technical Report NOS CO-OPS 067). Retrieved from <https://repository.library.noaa.gov/view/noaa/14420>.
- Olsen, A., Zhou, Q., Linde, J., & Arnbjerg-Nielsen, K. (2015). Comparing Methods of Calculating Expected Annual Damage in Urban Pluvial Flood Risk Assessments. *Water*, 7(12), 255–270. <https://doi.org/10.3390/w7010255>
- Pachauri, R. K., Allen, M. R., Barros, V. R., Broome, J., Cramer, W., Christ, R., ... Dasgupta, P. (2014). *Climate change 2014: synthesis report. Contribution of Working Groups I, II and III to the fifth assessment report of the Intergovernmental Panel on Climate Change*. IPCC.
- Pour, S. H., Wahab, A. K. A., Shahid, S., Asaduzzaman, M., & Dewan, A. (2020). Low impact development techniques to mitigate the impacts of climate-change-induced urban floods: Current trends, issues and challenges. *Sustainable Cities and Society*, 62, Article 102373. <https://doi.org/10.1016/j.scs.2020.102373>
- Rahmstorf, S., Cazenave, A., Church, J. A., Hansen, J. E., Keeling, R. F., Parker, D. E., & Somerville, R. C. J. (2007). Recent Climate Observations Compared to Projections. *J Science*, 316(5825), 709. <https://doi.org/10.1126/science.1136843>. -709.
- Sahin, O., & Mohamed, S. (2013). A spatial temporal decision framework for adaptation to sea level rise. *Environmental Modelling & Software*, 46, 129–141. <https://doi.org/10.1016/j.envsoft.2013.03.004>
- Saltelli, A., & Annoni, P. (2010). How to avoid a perfunctory sensitivity analysis. *Environmental Modelling & Software*, 25, 1508–1517. <https://doi.org/10.1016/j.envsoft.2010.04.012>
- Yamashita, Sampa, Watanabe, Ryoichi, & Shimatani, Y. (2016). Smart adaptation activities and measures against urban flood disasters. *Sustainable Cities and Society*, 27, 175–184. <https://doi.org/10.1016/j.scs.2016.06.027>
- Scawthorn, C., Blais, N., Seligson, H., Tate, E., Mifflin, E., Thomas, W., ... Jones, C. J. N. H. R. (2006). HAZUS-MH flood loss estimation methodology. I: Overview and flood hazard characterization, 7(2), 60–71.
- Sweet, W., Kopp, R. E., Weaver, C. P., Obeyseker, J. T. B., Horton, R. M., Thieler, E. R., & Zervas, C. E. (2017). Global and regional sea level rise scenarios for the United States. doi:<https://doi.org/10.7289/v5/tr-nos-coops-083>.
- Sweet, W. V., Kopp, R. E., Weaver, C. P., Obeyseker, J., Horton, R. M., Thieler, E. R., & Zervas, C. (2017). *Global and Regional Sea Level Rise Scenarios for the United States*. NOAA Technical Report NOS CO-OPS 083. Retrieved from.
- Torabi, E., Dedekorkut-Howes, A., & Howes, M. (2018). Adapting or maladapting: Building resilience to climate-related disasters in coastal cities. *Cities*, 72, 295–309. <https://doi.org/10.1016/j.cities.2017.09.008>
- Vitousek, S., Barnard, P. L., Fletcher, C. H., Frazer, N., Erikson, L., & Storlazzi, C. D. (2017). Doubling of coastal flooding frequency within decades due to sea-level rise. *Scientific Reports*, 7. <https://doi.org/10.1038/s41598-017-01362-7>
- Willows, R., Reynard, N., Meadowcroft, I., & Connell, R. (2003). Climate adaptation: Risk, uncertainty and decision-making. *UKCIP Technical Report: UK Climate Impacts Programme*.
- Xian, S. Y., Lin, N., & Hatzikyriakou, A. (2015). Storm surge damage to residential areas: a quantitative analysis for Hurricane Sandy in comparison with FEMA flood map. *Natural Hazards*, 79(3), 1867–1888. <https://doi.org/10.1007/s11069-015-1937-x>
- Yang, D. Y., & Frangopol, D. M. (2020). Risk-Based Vulnerability Analysis of Deteriorating Coastal Bridges under Hurricanes Considering Deep Uncertainty of Climatic and Socioeconomic Changes. *ASCE-ASME Journal of Risk and Uncertainty in Engineering Systems, Part A: Civil Engineering*, 6(3), Article 04020032. <https://doi.org/10.1061/AJRUA6.0001075>
- Yohe, G., Knee, K., & Kirshen, P. (2011). On the economics of coastal adaptation solutions in an uncertain world. *Climatic Change*, 106(1), 71–92. <https://doi.org/10.1007/s10584-010-9997-0>
- Zarekarizi, M., Srikrishnan, V., & Keller, K. (2020). Neglecting uncertainties biases house-elevation decisions to manage riverine flood risks. *Nature Communications*, 11 (1), 5361. <https://doi.org/10.1038/s41467-020-19188-9>
- Zhang, P., & Peeta, S. (2011). A generalized modeling framework to analyze interdependencies among infrastructure systems. *Transportation Research Part B: Methodological*, 45(3), 553–579. <https://doi.org/10.1016/j.trb.2010.10.001>